DEM GENERATION FROM HIGH RESOLUTION SATELLITE IMAGERY USING PARALLEL PROJECTION MODEL

A. Habib, E. M. Kim, M. Morgan, I. Couloigner

Department of Geomatics Engineering, University of Calgary,
Calgary, 2500 University Drive NW, Calgary, AB, T2N 1N4, Canada
(habib@geomatics.ucalgary.ca, emkim@ucalgary.ca, mfmorgan@ucalgary.ca, couloigner@geomatics.ucalgary.ca)

TS: HRS DEM Generation from SPOT-5 HRS Data

KEY WORDS: SPOT, High resolution, Satellite, Push Broom, Modelling, DEM, Stereoscopic, Matching

ABSTRACT:

DEM generation from stereoscopic imagery is contingent on establishing the mathematical model relating the scene coordinates of conjugate points to the ground coordinates of the corresponding object point. Either rigorous or approximate models can be used to establish such a relationship. Rigorous modelling necessitates a full understanding of the imaging geometry associated with the involved sensor. Moreover, it involves the external characteristics (as represented by the Exterior Orientation Parameters – EOP) and the internal characteristics (as represented by the Interior Orientation Parameters – IOP) of the imaging sensor. Such characteristics are derived with the help of control information, which might take the form of a calibration test field, ground control points, and/or onboard navigation units (e.g., GPS/INS). However, the derivation of these parameters might not be always possible due to: the lack of sufficient control; weak imaging geometry (especially for satellite imaging systems with narrow angular field of view); and/or intentional concealment by the data provider (e.g., Space Imaging does not release the IOP and the EOP for their commercially available imagery). Therefore, there has been an increasing interest to investigate approximate models, which do not explicitly involve the internal and external characteristics of the imaging system. Among them, parallel projection has become a popular model for its simplicity and accurate representation of imaging sensors with narrow angular field of view, which is the case for newly launched high resolution satellite imagery (e.g., IKONOS, QUICKBIRD, SPOT-5, ORBVIEW, and EOS-1). This paper presents a complete methodology for DEM generation from stereo-satellite scenes using parallel projection modelling of the imaging geometry. The performance of the developed methodology is evaluated through real datasets captured by SPOT-1, SPOT-2, and SPOT-5.

1. INTRODUCTION

DEM generation from remotely sensed imagery is crucial for a variety of mapping applications such as ortho-photo generation, city modelling, object recognition, and creation of perspective views. Recently launched high resolution imaging satellites (e.g., SPOT-5, IKONOS, QUICKBIRD, ORBVIEW, and EOS-1) constitute an excellent source for efficient, economic, and accurate generation of DEM data for extended areas of Earth's surface. In general, the procedure for DEM generation from stereoscopic views can be summarized as follows (Shin et al., 2003):

- Feature selection in one of the scenes of a stereo-pair: Selected features should correspond to an interesting phenomenon in the scene and/or the object space.
- Identification of the conjugate feature in the other scene: This problem is known as the matching/correspondence problem within the photogrammetric and computer vision communities.
- Intersection procedure: Matched points in the stereo-scenes undergo an intersection procedure to produce the ground coordinates of corresponding object points. The intersection process involves the mathematical model relating the scene and ground coordinates.
- Point densification: High density elevation data is generated within the area under consideration through an interpolation in-between the derived points in the previous step.

The matching problem and the mathematical model relating the scene and ground coordinates of corresponding points are the most difficult problems associated with DEM generation from high resolution imaging satellites. To ensure a reliable solution of the matching problem, prominent features, as represented by an interesting signal around the selected primitives, are usually used (Tomasi et al., 1991; Harris et al., 1988; Förstner, 1986). Restricting the search space, where conjugate points are sought for, is another factor that can be used to reduce matching ambiguities. Generating normalized scenes (i.e., resampled scenes according to epipolar geometry) is the most common approach for restricting the search space for conjugate points (Cho et al., 1992). In normalized scenes, conjugate points are expected to lie along the same row in overlapping scenes.

The mathematical relationship between the scene and object coordinates of conjugate points can be established using either rigorous or approximate modelling of the perspective geometry of the imaging system. Rigorous modelling requires a comprehensive understating of the imaging geometry. In this type of modelling, the IOP as well as the EOP of the imaging system are explicitly involved in the mathematical relationship between corresponding scene and object coordinates (Habib and Beshah, 1998). Deriving such characteristics requires the availability of control information, which might be in the form of a calibration test field, ground control points, and/or onboard navigation units (GPS/INS). However, deriving such parameters might be hindered by: the lack of sufficient control; weak imaging geometry (e.g., narrow angular field of view of the imaging sensor); and/or intentional concealment of these parameters by the data provider (e.g., Space Imaging does not provide the IOP and the EOP for their commercially available IKONOS imagery). Therefore, there has been an increasing

interest within the photogrammetric community to adopt approximate models since they require neither a comprehensive understanding of the imaging geometry nor the internal and external characteristics of the imaging sensor. Approximate models include Direct Linear Transformation (DLT), self-calibrating DLT (SDLT), Rational Function Model (RFM), and parallel projection (Vozikis et al., 2003; Fraser, 2000; OGC, 1999; Ono et al., 1999; Wang, 1999; Gupta et al., 1997; El-Manadili and Novak, 1996). Among these models, parallel projection is gaining popularity for its simplicity and accurate representation of the perspective geometry associated with scenes captured by a narrow angular field of view imaging sensor that is travelling with constant velocity and constant attitude. Another motivation for utilizing the parallel projection is the straightforward procedure for generating normalized imagery, which is necessary for increasing the reliability and reducing the search space associated with the matching problem (Morgan et al., 2004).

In this paper, the parallel projection will be used for representing the perspective geometry and deriving a DEM from high resolution satellite imagery. The following section presents a brief overview of the parallel projection formulation as well as the generation of resampled scenes according to epipolar geometry. Section 3 explains the DEM generation methodology including primitive extraction, matching, space intersection, and interpolation. This is followed by a description of the incorporated real datasets captured by SPOT-1, SPOT-2, and SPOT-5 as well as an evaluation of the performance of proposed methodology for DEM generation in sections 4 and 5, respectively. Finally, conclusions and recommendations for future work are summarized in section 6.

2. PARALLEL PROJECTION: BACKGROUND

High resolution imaging satellites (e.g., IKONOS, SPOT, QUICKBIRD, ORBVIEW, and EOS-1) constitute an efficient and economic source for gathering current data pertaining to an extended area of the surface of the Earth. Due to technical limitations, two dimensional digital arrays that are capable of capturing imagery with geometric resolution, which is commensurate to that associated with traditional analogue cameras, are not yet available. Therefore, high resolution imaging satellites implement a linear array scanner in their focal plane. Successive coverage of contiguous areas on the Earth's surface is achieved through multiple exposures of this scanner during the system's motion along its trajectory. For systems moving with constant velocity and attitude, the imaging geometry can be described by a perspective projection along the scanner direction and parallel projection along the system's trajectory. Moreover, for imaging systems with narrow angular field of view, the imaging geometry can be further approximated with a parallel projection along the scanner direction.

The smooth trajectories and narrow angular field of view associated with high resolution imaging satellites (e.g., the angular field of view for IKONOS is less than one degree) contribute towards the validity of the parallel projection as a highly suitable model for representing the mathematical relationship between corresponding scene and object coordinates. The following subsections present a brief overview of the formulation of the parallel projection model. Also, the conceptual procedure for resampling satellite scenes according to epipolar geometry (i.e., normalized scene generation) is summarized.

2.1 Parallel Projection: Mathematical Model

The parallel projection model involves eight parameters: two parameters for the projection direction – L, M, three rotation angles – ω, φ, κ, two shifts – Δx, Δy, and one scale factor – s (Ono et al., 1999). The non-linear form of the parallel projection can be re-parameterized to produce the linear form, as expressed in Equation 1.

$$\begin{aligned} x &= A_1X + A_2Y + A_3Z + A_4 \\ y &= A_5X + A_6Y + A_7Z + A_8 \end{aligned} \tag{1}$$

where:

x, y are the scene coordinates,

X, Y, Z are the object coordinates of the corresponding object point, and

$A_1 \sim A_8$ are the re-parameterized parallel projection parameters.

The imaging geometry of scenes captured by an imaging scanner moving along a straight line trajectory with constant velocity and attitude can be described by a parallel projection along the flight trajectory and perspective geometry along the scanner direction. The perspective projection along the scanner direction can be approximated by a parallel projection for systems with narrow angular field of view. However, additional term (ψ) is introduced in the y-equation to make the projection along the scanner direction closer to being a parallel one, Equation 2 (Morgan et al., 2004).

$$\begin{aligned} x &= A_1X + A_2Y + A_3Z + A_4 \\ y &= \frac{A_5X + A_6Y + A_7Z + A_8}{1 + \frac{\tan(\psi)}{c}\left(A_5X + A_6Y + A_7Z + A_8\right)} \end{aligned} \tag{2}$$

where:

c is the scanner principal distance, and

ψ is the scanner roll angle.

The parameters ($A_1 \sim A_8$, ψ) can be estimated for each scene if at least five ground control points (GCP) are available.

2.2 Normalized Scene Generation

In addition to the simplicity of the parallel projection model, it allows for resampling the involved scenes according to epipolar geometry. Such a resampling is known as normalized scene generation. The normalization process is beneficial for DEM generation since the search space for conjugate points can be reduced from 2-D to 1-D along the epipolar lines as represented by the same rows in the transformed scenes. The resampling process can be summarized as follows, refer to (Morgan et al., 2004) for more technical details:

- The parallel projection parameters ($A_1 \sim A_8$, ψ), Equations 2, are determined for the left and right scenes using some ground control points.
- Derive the parallel projection parameters L, M, ω, φ, κ, Δx, Δy, and s that correspond to the estimated parameters ($A_1 \sim A_8$) in the previous step.
- Use the parallel projection parameters for the left and right scenes to derive an estimate of a new set of parameters for the normalized scenes. The newly derived parallel projection parameters will ensure the absence of y-parallax between conjugate points. Moreover, the x-parallax between conjugate points will be linearly proportional to the elevations of the corresponding object points.

- Use the parallel projection parameters for the original and normalized scenes to transform the grey values from the original scenes into the resampled scenes according to epipolar geometry.

3. DEM GENERATION

So far, the original scenes have been resampled according to epipolar geometry. The resampled scenes exhibit two main properties. First, conjugate points are located along the same rows. Second, the *x*-parallax between conjugate points is proportional to the height of the corresponding object point. The following subsections briefly discuss the utilization of the normalized imagery for DEM generation. The generation process involves four steps: primitive extraction, primitive matching, space intersection, and interpolation.

3.1 Primitive Extraction

At this stage, a decision has to be made regarding the primitives to be matched in the normalized scenes. Possible matching primitives include distinct points, linear features, and/or homogeneous regions. The choice of the matching primitives is crucial for ensuring the utmost reliability of the outcome from the DEM generation process. In this research, point features are chosen. This choice is motivated by the fact that the parallel projection model, which will be used for space intersection, can only deal with point primitives.

Förstner interest operator (Förstner, 1986) is used to extract distinct points from the imagery. The operator identifies points with unique grey value distribution at their vicinity (e.g., corner points and blob centres), thus reducing possible matching ambiguities (refer to Figures 5 and 6 for a sample of the extracted points). The next section discusses the matching procedure of these points.

3.2 Primitive Matching

The outcome from the interest operator is a list of distinct points in the left and right scenes. This section deals with the identification of conjugate points, which is known as the matching/correspondence problem. The solution to this problem can be realized through defining the location and the size of the search space as well as establishing matching criteria for evaluating the degree of similarity between conjugate points.

3.2.1 Centre of Search Space

The search space outlines the area where conjugate points to the selected matching primitives are expected. For normalized scenes, conjugate points should lie along the same rows. The relative location between conjugate points along the epipolar lines as described by the x-parallax depends on the height of the corresponding object point. An approximate value for the x-parallax can be derived by knowing the average height associated with the area under consideration.

3.2.2 Size of the Search Space

For normalized imagery, the size of the search space in the right scene across the epipolar lines should be exactly equal to the size of the template centred at the matching primitive in the left scene. In other words, the search is done in one direction along the epipolar lines as represented by the rows of the normalized scenes. However, since there is no guarantee that the y-parallax between conjugate points in the normalized scenes is exactly zero, the size of the search space across the rows is selected to be slightly larger than the size of the template.

On the other hand, the size of the search space along the rows depends on the height variation within the imaged area. Rugged terrain would require a wider search space compared to that associated with relatively flat terrain.

3.2.3 Matching Criteria

The matching criteria deal with establishing a quantitative measure that describes the degree of similarity between a template in the left scene and a matching window, of the same size, within the search space in the right scene. Either correlation coefficient or least squares matching could be used to derive such a similarity measure. Since the involved imagery is captured by the same platform within a short time period, one should not expect significant variation in the appearance of conjugate features in the acquired scenes. Therefore, we used the correlation coefficient for deriving the similarity measure between selected features in the left scene and hypothesized matching candidates in the right scene. The centre of the matching window that yields the highest correlation coefficient, which is larger than a predefined threshold (e.g., 0.7), is chosen as the initial match of the selected point in the left scene.

To eliminate possible mismatches, initially matched points undergo a consistency check using neighbouring matches. More specifically, the *x*-parallax (P_x) value of a matched point is compared to those associated with the surrounding matched points. For a given point, the mean and standard deviation of the *x*-parallax values of the neighbouring points (i.e., μ and σ, respectively) are computed. Then, if the *x*-parallax for that point is significantly different from those associated with neighbouring points (e.g., $\frac{|Px - \mu|}{\sigma} > Threshold$), the point is highlighted as a mismatch and is eliminated.

3.3 Space Intersection

Following the matching process, conjugate points undergo an intersection procedure to derive the ground coordinates of the corresponding object points. The parallel projection formulas (Equations 2) are used for such computation. For a conjugate pair in the left and right scenes, one can formulate four equations with three unknowns (*X*, *Y*, *Z* - the ground coordinates of the corresponding object point). These coordinates can be derived through a least-squares adjustment procedure.

3.4 Interpolation

So far, the ground coordinates of matched interest points, which passed the consistency check, are derived through space intersection. These points are irregularly distributed and are not dense enough to represent the object space. Therefore, they need to be interpolated. In this research, Kriging is used to interpolate the resulting object space points into regular grid. The Kriging methodology derives an estimate of the elevation at a given point as a weighted average of the heights at neighbouring points. However, the weights are stochastically derived based on the statistical properties of the surface as described by the elevations at the matched interest points (Allard, 1998).

So far, we outlined a comprehensive methodology for DEM generation from high-resolution satellite scenes using an approximate model.. The reliability of the matching process is enhanced by utilizing scenes that are resampled according to epipolar geometry. The following sections deal with experimental results from real datasets to evaluate the validity and the performance of the developed methodology.

4. DATASET DESCRIPTION

High resolution SPOT scenes captured by SPOT-1, SPOT-2, and SPOT-5 are used for evaluating the performance of the proposed methodology for scene resampling according to epipolar geometry as well as DEM generation. The following subsections present a brief overview of these datasets as well as some of the associated metadata.

4.1 Dataset 1

The first dataset involves a stereo-pair captured by SPOT-1 and SPOT-2 over Korea, Figure 1. The specifications of these scenes are listed in Table 1. As mentioned earlier, normalized scene generation requires a minimum of five ground control points to estimate the parallel projection parameters (Equation 2). For this dataset, a total of twenty-six ground control points have been collected through a triangulation procedure involving aerial imagery over the same area.

4.2 Dataset 2

A stereo-pair captured by SPOT-5 over Belgium, © CNES (2003), distributed by Spot Image – all rights reserved, Figure 2, has been used. The scenes have been provided by HRS instruments as part of the Scientific Assessment Program (ASP) to evaluate the quality of derived DEM data from SPOT-5. The metadata associated with this dataset is provided in Table 2. A total of nine ground control points have been collected to estimate the parallel projection parameters. The ground coordinates of these points are derived through a terrestrial GPS survey by the University of Liège, Belgium.

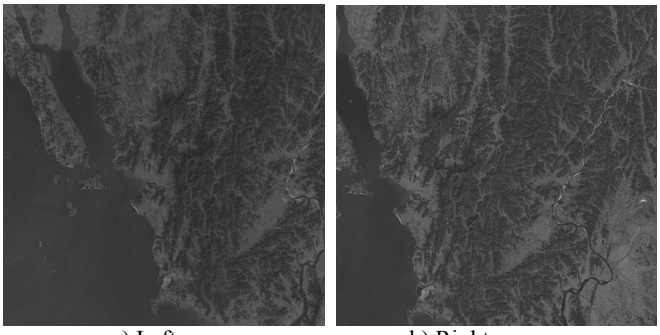

a) Left scene b) Right scene

Figure 1: Original scenes for the first dataset

Scene	Left	Right
Satellite ID	SPOT-1 (level 1A)	SPOT-2 (level 1A)
Focal length (mm)	1082	1082
Date of capture	1998-10-29	1998-10-29
Time of capture	02:37:26.2	02:06:47.4
Pixel size (mm)	0.013	0.013
# of rows and columns	6000 ×6000	6000 ×6000
Incident angle (°)	20.2	-29.7
Ground pixel (m)	10	10

Table 1: Specifications of the first dataset

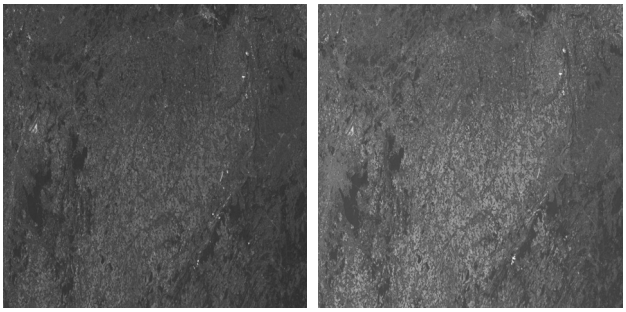

a) Left scene b) Right scene

Figure 2: Original scenes for the second dataset

Scene	Left	Right
Satellite ID	SPOT-5 (level 1A)	SPOT-5 (level 1A)
Focal length (mm)	1082	1082
Date of capture	2002-09-24	2002-09-24
Time of capture	10:53:07	10:54:39
Pixel size (mm)	0.0065	0.0065
# of rows and columns	12000 ×12000	12000 ×12000
Incidence angle (°)	23.031638	-22.471756
Ground pixel (m)	5	5

Table 2: Specifications of the second dataset

5. EXPERIMENTAL RESULTS

The proposed methodology starts by using a subset of the provided control points to estimate the parallel projection parameters in Equation 2. For the first dataset, six ground control points are used for parameter estimation, while the remaining twenty points are used as check points. Similarly, a total of six ground control points are used to derive the parallel projection parameters for the second dataset, while the remaining three points are used as check points. The square root of the resulting variance component ($\hat{\sigma}_0$) from the adjustment procedure for the first and second datasets are listed in Tables 3 and 4, respectively. The variance component represents the quality of fit of the observed scene and ground coordinates of the involved points to the parallel projection model, as described by Equations 2. Based on the numbers in Tables 3 and 4 (approximately one-third and four pixels for the first and second dataset, respectively), one can conclude that the first dataset shows a better fit. The poor fit associated with the second dataset can be attributed to inferior quality of the provided control and/or problems during the data acquisition process.

Following the estimation of the parallel projection parameters, the outlined methodology in section 2.2 has been used to generate normalized scenes according to epipolar geometry. The normalized scenes are generated to ensure the absence of any y-parallax between conjugate points. The mean value of the absolute y-parallax associated with the control and check points for the first and second datasets are shown in Tables 3 and 4, respectively. Closer inspection of these values verifies the success of the proposed methodology in eliminating the y-parallax between conjugate points. A stereo-anaglyph covering the overlapping area in the second dataset is shown in Figure 3. Three-dimensional visualization of this figure supports the feasibility of using the parallel projection model for normalized scene generation.

Finally, the normalized scene coordinates as well as the derived parallel projection parameters for the normalized scenes are used in a space intersection procedure to derive the ground coordinates of corresponding object points. The derived ground coordinates for the check and control points, associated with the first and second datasets, are compared to the true values and reported in Tables 3 and 4, respectively. Similar to the analysis of the quality of fit, the first dataset is providing more accurate results (roughly half a pixel) when compared with the second one. The poor planimetric quality of the derived coordinates from the second dataset confirms the earlier prediction regarding a problem in the provided SPOT-5 data.

Parameter		Value
$\hat{\sigma}_0$ _Left scene (pixels)		0.3
$\hat{\sigma}_0$ _Right scene (pixels)		0.2
GCP errors	Mean $\lvert P_v \rvert$ (pixels)	0.0
	$\text{Mean}_{XY} \pm \text{Std}_{XY}$ (m)	0.000 ± 2.340
	$\text{Mean}_Z \pm \text{Std}_Z$ (m)	0.000 ± 0.858
Check points errors	Mean $\lvert P_v \rvert$ (pixels)	1.0
	$\text{Mean}_{XY} \pm \text{Std}_{XY}$ (m)	3.009 ± 6.520
	$\text{Mean}_Z \pm \text{Std}_Z$ (m)	2.895 ± 7.453

Table 3: Results for the first dataset

Parameter		Value
$\hat{\sigma}_0$ _Left scene (pixels)		3.7
$\hat{\sigma}_0$ _Right scene pixels)		3.9
GCP errors	Mean $\lvert P_v \rvert$ (pixels)	0.0
	$\text{Mean}_{XY} \pm \text{Std}_{XY}$ (m)	0.000 ± 18.605
	$\text{Mean}_Z \pm \text{Std}_Z$ (m)	0.000 ± 2.385
Check points errors	Mean $\lvert P_v \rvert$ (pixels)	0.0
	$\text{Mean}_{XY} \pm \text{Std}_{XY}$ (m)	31.436 ± 64.985
	$\text{Mean}_Z \pm \text{Std}_Z$ (m)	4.610 ± 7.623

Table 4: Results for the second dataset

Since this study is mainly focusing on the evaluation of the quality of derived DEMs from SPOT-5 scenes, the remainder of the experimental results section is dedicated to the scenes captured over Belgium, dataset 2. A sub-region from the normalized scenes has been cropped as shown in Figure 4. The DEM generation process starts with the application of Förstner interest operator to extract distinct points from the sub-scenes. A sample of the extracted points can be seen in Figures 5 and 6. The extracted points are then used as candidates for the matching procedure according to the proposed strategy in section 3. The results of the matching process have been visually inspected and we found out that only five points out of 1876 were wrongly matched (a success rate of 99.7%). Figures 5 and 6 show samples of correctly and wrongly matched points, respectively.

Finally, the derived ground coordinates are used in an interpolation procedure to produce a high density DEM over the area shown in Figure 4. A shaded relief view of such DEM is displayed in Figure 7.

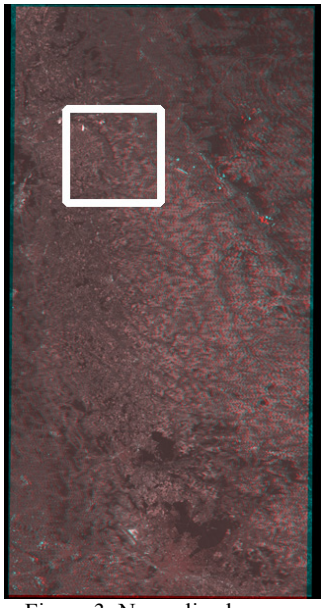

Figure 3: Normalized scenes (12146×6416) for dataset 2

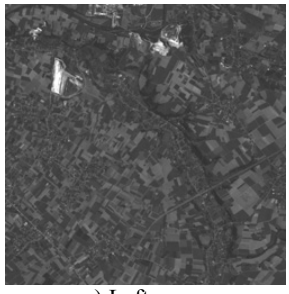

a) Left scene

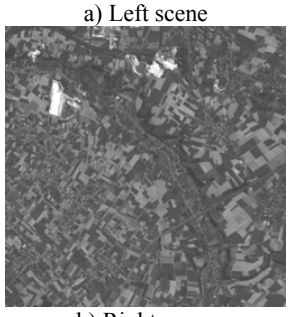

b) Right scene

Figure 4: Cropped normalized scenes

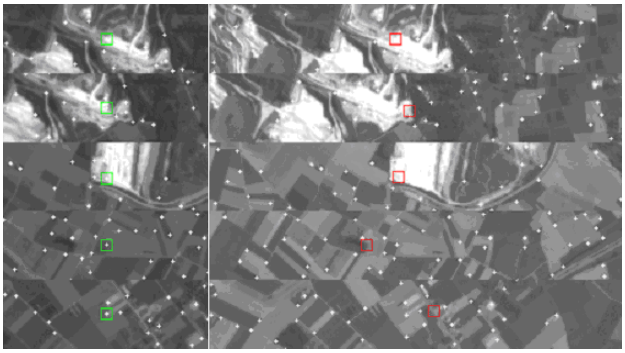

Figure 5. Examples of mismatched points as represented by the centres of boxes in the left and right scenes

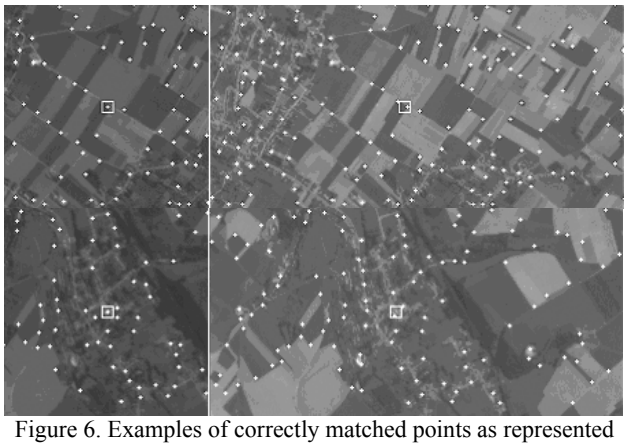

Figure 6. Examples of correctly matched points as represented by the centres of boxes in the left and right scenes

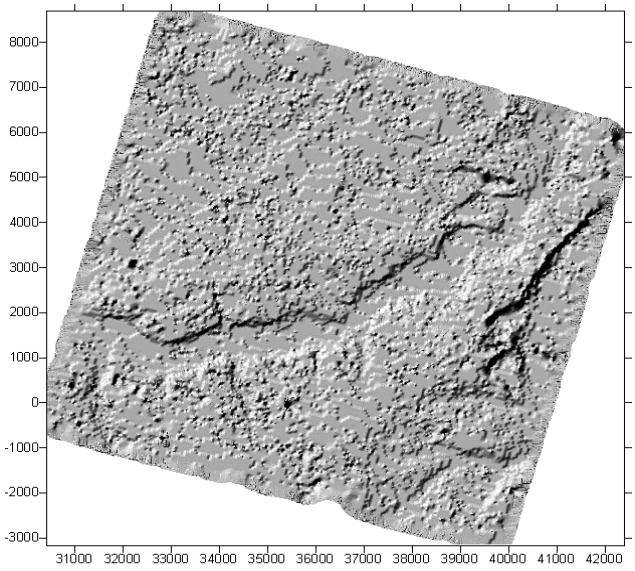

Figure 7. A shaded relief of the generated DEM

6. CONCLUSIONS AND RECOMMENDATIONS

In this paper, we presented a comprehensive methodology for DEM generation from scenes captured by high resolution imaging satellites. The proposed methodology has two main characteristics. Firstly, the parallel projection has been used as the mathematical model approximating the relationship between corresponding scene and ground coordinates. The validity of this model is attributed to the fact that the imaging geometry of a narrow angular field of view scanner, moving with a constant velocity and attitude, resembles a parallel projection. In this regard, one should mention that the derivation of the parallel projection parameters does not require the knowledge of the internal and external characteristics of the imaging system. The involved parameters can be derived through a minimum of five ground control points. Secondly, the parallel projection model can be used to generate normalized scenes (i.e., resampled imagery according to epipolar geometry). The generation of normalized scenes is advantageous for DEM generation since it reduces the search space for conjugate points into 1-D along the epipolar lines as represented by corresponding rows.

The resampled scenes are manipulated by an interest operator to extract point primitives with a unique grey value distribution at their vicinity. These points are then considered as candidates for the matching process, where the correlation coefficient has been used to evaluate the degree of similarity between hypothesized matches within the involved scenes. Matched points are projected into the object space using an intersection procedure. Finally, derived object points undergo an interpolation procedure to produce a dense DEM over the area in question.

Reported results from real datasets verified the validity of the developed approach for normalized scene generation, where almost zero y-parallax is observed between conjugate points. The derived ground coordinates from the SPOT-1 and SPOT-2 data have been proven to be accurate within half a pixel. However, the derived ground coordinates from the SPOT-5 data have shown poorer performance, especially in the planimetric coordinates. Such inaccuracy can be either attributed to poor quality of the ground control points and/or problems with the data acquisition process.

Future research work will be focusing on further investigation into the SPOT-5 dataset to identify the cause of the poor quality of the derived ground coordinates. Moreover, we will derive a quantitative evaluation of the quality of the derived DEM by comparing it to LIDAR data over the same area.

REFERENCES

Allard, D., 1998, Geostatistical classification and class Kriging, *Journal of Geographic Information and Decision Analysis*, 2(2), 77-90.

Cho, W., T. Schenk, and M. Madani, 1992. Resampling Digital Imagery to Epipolar Geometry, *IAPRS International Archives of Photogrammetry and Remote Sensing*, 29(B3): 404-408.

El-Manadili, Y., and K. Novak, 1996. Precision Rectification of SPOT Imagery Using the Direct Linear Transformation Model, *Photogrammetric Engineering & Remote Sensing*, 62(1): 67-72.

Förstner, W., 1986. A Feature Based Correspondence Algorithm for Image Matching, *International Archives of Photogrammetry*, 26(3): 1-16.

Fraser, C., 2000. High Resolution Satellite Imagery : A Review of Metric Aspects, *IAPRS International Archives of Photogrammetry and Remote Sensing*, Vol. 33, B7, 452-459.

Gupta, R. and R. Hartley, 1997. Linear Pushbroom Cameras, *IEEE Transactions on Pattern Analysis and Machine Intelligence*, 189(9): 963-975.

Habib, A., and B. Beshah, 1998. Multi Sensor Aerial Triangulation. *ISPRS Commission III Symposium*, Columbus, Ohio, 6 – 10 July, 1998.

Harris, C. and M. Stephens, 1988. A Combined Corner and Edge Detector, *Fourth Alvey Vision Conference*, 147-151.

Morgan, M., K. Kim, S. Jeong, and A. Habib, 2004. Indirect Epipolar Resampling of Scenes Using Parallel Projection Modeling of Linear Array Scanners, *XXth Congress of ISPRS*, 12-23 July, 2004.

OGC (OpenGIS Consortium), 1999. The OpenGIS Abstract Specification – Topic 7: The Earth Imagery Case. http://www.opengis.org/public/abstract/99-107.pdf (accessed 1 April 2004)

Ono, T., Y. Honmachi, and S. Ku, 1999. Epipolar Resampling of High Resolution Satellite Imagery, *Joint Workshop of ISPRS WG I/1, I/3 and IV/4 Sensors and Mapping from Space*.

Shin, D., H. Lee, and P. Wonkyu, 2003. Stereroscopic GCP Simulation Model for the Assessement of Camera Modeling Algorithms, *ISSDQ Proceedings*, Hongkong, China,

Tomasi, C., and T. Kanade, 1991. *Detection and Tracking of Point Features,* Carnegie Mellon University Technical Report CMU-CS-91-132.

Vozikis, G., C. Fraser, and J. Jansa, 2003. Alternative Sensor Orientation Models for High Resolution Satellite Imagery, *Publikationen der Deutschen Gesellschaft für Photogrammetrie, Fernerkundung und Geoinformation*, Bochum, 179- 186.

Wang, Y., 1999. Automated Triangulation of Linear Scanner Imagery, *Joint Workshop of ISPRS WG I/1, I/3 and IV/4, Sensors and Mapping from Space*, Hanover, September, 27-30.